2024 년 2 월
석사학위 논문

Regulation of Cell Adhesion by RapB and Roles of NHE1 in Cell Migration and Phagocytosis

조 선 대 학 교 대 학 원

글로벌바이오융합학과

한 우 리

Regulation of Cell Adhesion by RapB and Roles of NHE1 in Cell Migration and Phagocytosis

RapB 단백질에 의한 세포부착 조절 및 세포이동과 식균작용에서의 **NHE1** 단백질의 역할 연구

2024 년 **2** 월 **23** 일

조 선 대 학 교 대 학 원

글로벌바이오융합학과

한 우 리

Regulation of Cell Adhesion by RapB and Roles of NHE1 in Cell Migration and Phagocytosis

지도교수 전 택 중

이 논문을 이학석사학위 신청 논문으로 제출함

2023 년 10 월

조 선 대 학 교 대 학 원

글로벌바이오융합학과

한 우 리

한우리의 석사학위논문을 인준함

위원장 조광원 (인)

위 원 이준식 (인)

위 원 전택중 (인)

2023 년 12 월

조 선 대 학 교 대 학 원

CONTENTS

LIST OF FIGURES

PART I. RapB inhibits cell migration through strong cell adhesion.

PART II. Roles of NHE1 in cell migration and phagocytosis in *Dictyostelium*.

LIST OF TABLES

ABBREVIATIONS

cAMP	Cyclic adenosine monophosphate
DAPI	4’,6’-diamidine-2’-phenylidole dihydrochloride
DC	Direct current
ECM	Extra cellular matrix
EF	Electric Field
GAP	GTPase activating proteins
GDP	Guanosine diphosphate
GFP	Green fluorescent protein
GEF	Guanine nucleotide exchange factor
GTP	Guanosine triphosphate
NHE1	Sodium-hydrogen exchanger 1
PBS	Phosphate-buffered saline
PCR	Polymerase chain reaction
SD	Standard deviation
SEM	Standard error of measurement

ABSTRACT

Regulation of Cell Adhesion by RapB and Roles of NHE1 in Cell Migration and Phagocytosis

Uri Han

Advisor: Prof. Taeck Joong Jeon, Ph.D.

Department of Life Science

Graduate School of Chosun University

Ras proteins are small monomeric GTPases acting as molecular switches in various cellular signaling pathways, including cell migration, polarity, differentiation, and apoptosis. There are three Rap proteins (RapA, RapB, and RapC) in *Dictyostelium.* RapA, the closest homolog of human K-Ras, plays an essential role in integrin-mediated cell-substrate adhesion, cadherin-mediated cell-cell adhesion, cell migration, and proliferation. It has been reported that RapC has opposite functions to RapA in cell migration and adhesion and plays an unique important role in multi-tip formation in multicellular development of the cells. Contrary to RapA and RapC, RapB remains uncharacterized yet though RapB has high homology to RapA (Rap1). To investigate the functions of RapB, cells with deletion of the *rapB* gene were generated using the CRISPR/Cas9 gene editing system. Using the *rapB* mutated cells (*rapB* null), I examined the phenotypes of the cells in cell adhesion and migration. *rapB* null cells showed decreased cell size and adhesion strength compared to wild-type cells. In chemotaxis using cAMP as a chemoattractant, *rapB* null cells showed increased migration speed toward chemoattractants. These phenotypes were rescued by expression of RapA as well as by expression of RapB, but not by RapC. These results suggest that RapB has an inhibitory function in chemoattractant-mediated cell migration possibly through controlling cell-substrate adhesion. These

functions of RapB in regulating cell migration and adhesion are similar to those of RapA but opposite to those of RapC.

NHE1 is a sodium-hydrogen antiporter located in the plasma membrane of cells. In *Dictyostelium discoideum*, NHE1 plays an essential role in maintaining cell polarity and intracellular pH homeostasis. NHE1 regulates migration speed and orientation of cells in chemotaxis through regulation of cell polarity. To determine whether NHE1 plays a similar role in elecrtoraxis as in chemotaxis, I investigated directional cell migration in response to electric fields (EF). Electrotaxis was performed using vegetative cells or aggregation-competent cells. Vegetative *nhe1* null cells exhibited decreased migration speed and directionality in both electrotaxis and chemotaxis using folates, which are secreted by the bacteria, as chemoattractants. Using the intracellular calcium marker GCaMP3, I confirmed the intracellular calcium level of cells. *nhe1* null cells showed delayed calcium elevation kinetics in response to folic acid, suggesting that NHE1 might be involved in phagocytosis which are mediated by folic acid secreted by bacteria. As expected, cells lacking NHE1 showed slower growth rate and smaller colonies on the bacteria growing plates, compared to wild-type cells. These results suggest that NHE1 plays an important role in regulating migration speed and directionality in both electrotaxis and chemotaxis in the vegetative state. In addition, NHE1 appears to be involved in the regulation of phagocytosis.

.

국문초록

RapB 에 의한 세포 부착 조절과 세포 이동 및 식균 작용에서 NHE1 의 역할

한 우 리

지도교수: 전 택 중

글로벌바이오융합학과

조선대학교 대학원

Ras 단백질은 세포 이동, 극성, 분화 및 세포 사멸을 포함한 다양한 세포 신호 경로에서 분자적 스위치 역할을 하는 작은 단량체 GTPase입니다. *Dictyostelium*에는 세 개의 Rap 단백질 (RapA, RapB, 그리고 RapC)이 있습니다. 인간의 K-Ras와 가장 가까운 상동체인 RapA는 integrin 매개 세포-기질 부착, cadherin 매개 세포간 부착, 세포 이동 및 증식에 필수적인 역할을 합니다. RapC는 세포 이동 및 부착에서 RapA와 상반된 기능을 하며, 세포의 다세포 발달에서 다중 팁 형성에 독특하고 중요한 역할을 하는 것으로 보고되었습니다. RapB는 RapA와 RapC와는 달리 RapA(Rap1)와 높은 상동성을 가지고 있음에도 불구하고 아직까지 그 기능이 밝혀지지 않은 상태입니다. RapB의 기능을 조사하기 위해 크리스퍼 유전자가위(CRISPR/Cas9) 시스템을 이용하여 *rapB* 유전자가 결실된 세포를 제작하였습니다. *rapB* 돌연변이 세포 (*rapB* 결손 세포)를 이용해 세포 부착과 이동에 있어 세포의 표현형을 확인한 결과, *rapB* 결손 세포는 야생형 세포에 비해 세포 크기와 부착 강도가 감소한 것으로 나타났습니다. 화학유인물질로 cAMP를 사용한 주화성 이동에서 *rapB* 결손 세포는 화학유인물질을 향한 이동속도가 증가했습니다.

이러한 표현형은 RapA의 발현과 RapB의 발현에 의해 회복되었지만, RapC의 발현에 의해 회복되지는 않았습니다. 이러한 결과는 RapB가 세포-기질 부착을 제어함으로써 화학유인물질 매개 세포 이동을 억제하는 기능을 가지고 있음을 시사합니다. 세포 이동과 부착을 조절하는 RapB의 이러한 기능은 RapA와 유사하지만 RapC와는 반대입니다.

NHE1은 세포의 원형질막에 위치한 나트륨-수소 역수송체입니다. *Dictyostelium discoideum*에서 NHE1은 세포 극성 및 세포 내 pH 항상성을 유지하는데 필수적인 역할을 합니다. NHE1은 세포 극성 조절을 통해 세포의 이동 속도와 방향을 조절하여 세포의 주화성 이동을 조절합니다. NHE1이 주화성 이동과 마찬가지로 주전성 이동에서도 유사한 역할을 하는지 확인하기 위해, 전기장 (EF)에 반응하는 방향성 세포 이동을 조사하였습니다. 발달상태의 세포 또는 응집 능력이 있는 세포를 이용하여 주전성 이동을 수행하였습니다. 발달상태의 *nhe1* 결실 세포는 주전성 이동과 박테리아가 분비하는 엽산을 화학유인물질로 이용한 주화성 이동 모두에서 이동 속도와 방향성이 감소하는 것으로 나타났습니다. 세포 내 칼슘 마커 GCaMP3를 사용하여 세포 내 칼슘 수준을 확인하였습니다. *nhe1* 결실 세포는 엽산에 반응하여 칼슘 상승 역학이 지연되는 것으로 나타나 NHE1이 박테리아가 분비하는 엽산을 매개로 하는 식세포 작용에 관여할 수 있음을 시사하였습니다. 예상대로, NHE1이 결핍된 세포는 야생형 세포에 비해 성장 속도가 느리고 박테리아가 증식하는 플레이트에서 더 작은 콜로니를 보였습니다. 이러한 결과는 NHE1이 발달상태의 주전성 이동과 주화성 이동 모두에서 이동 속도와 방향성을 조절하는데 중요한 역할을 한다는 것을 시사합니다. 또한, NHE1은 식세포 작용의 조절에서 관여하는 것으로 보여집니다.

PART I. RapB inhibits cell migration through strong cell adhesion

I. Introduction

Many types of cells can sense various chemical signals that exist outside the cells, and the movement of cells by chemical signals is called 'chemotaxis' (Van Haastert and Devreotes, 2004; Jin, 2011). Chemotaxis is involved in many diverse physiological processes, including the recruitment of leukocytes to the sites of infection, tracking of lymphocytes in the human body, and neuronal patterning in the developments of nervous system. Misguided cell migration has implications in a variety of human diseases, including metastatic cancer and inflammatory diseases such as asthma and arthritis (Murphy, 2002; Jin et al., 2009; Jin et al., 2008). Chemokines which are a large family of small proteins acts as extracellular signals and the family of chemokine receptors, the G-protein-coupled receptors (GPCR), detect gradients of chemokines and guide the directed cell migration in vivo. However, the molecular mechanism how these receptors sense chemokine gradients and modulate the migration of immune and other cells is little known (Jin *et al.*, 2009). To understand the complicated biology of chemokines, it will also be important to understand the molecular mechanism of chemotaxis inherent in these cells more completely. Basic research in this field will provide the basis of knowledge necessary for the rational selection of targets requiring medical intervention and for the treatment of inflammatory diseases, autoimmune diseases and immunodeficiencies (Jin *et al.*, 2008).

Research on chemotaxis in eukaryotes has progressed substantially through the study of neutrophils or the amoeba *Dictyostelium discoideum* as a model system (Van Haastert and Devreotes, 2004). *Dictyostelium* is a free-living soil amoeba. *Dictyostelium* cells detect the folic

acid, a chemoattractant secreted by bacteria, and chase the bacteria as a prey. When starvation occurs, cells tightly regulate the developmental processes. A single cell begins to secrete a chemoattractant cAMP, and surrounding cells detect this chemical signal and respond by chemotaxing toward the chemical source. In this process, chemotaxing cells secrete and detect cAMP on their own to form multicellular fruiting bodies. There are four cAMP receptors (cAR) have been identified in *Dictyostelium* (Kortholt and van Haastert, 2008). cAR1, one of the identified receptors, has a high affinity for cAMP and plays an essential role in signal transduction during early development and chemotaxis. *Dictyostelium* also contains one G-protein β subunit and one Gɣsubunit, which are both essential for chemotaxis. Of the 11 identified Gα subunits, Gα2 is coupled to the cAR1 receptor and most important for cAMP-mediated chemotaxis (Kumagai et al., 1991; Clapham and Neer, 1993). Recent studies, mostly performed in *Dictyostelium*, revealed that Ras subfamily proteins acts as key intermediates regulating directional sensing, cellular motility, and cell polarity in chemotaxis. (Charest and Firtel, 2007). The *Dictyostelium* Ras GTPase subfamily comprise 19 proteins; 15 Ras, 3 Rap, and one Rheb related protein (Kortholt and van Haastert, 2008).

Rap1(RapA) is the closest homolog of the closest homolog of human K-Ras. *Dictyostelium* Rap1, like Ras, cycles between an inactive GDP-bound and an active GTP-bound conformation. These inactivation and activation forms are regulated by guanine nucleotide exchange factors (GEFs) and GTPase activating proteins (GAPs), respectively (Bos, 2005). Similar to Ras, Rap1 protein plays as molecular switches to control a variety of cellular functions, including integrin-mediated cell adhesion, cadherin-based cell-cell adhesions, cell polarity, and cell survival (Lee and Jeon, 2012). Rap1 is rapidly and transiently activated in response to chemoattractant stimulation with a peak at 5-10 sec and activated Rap1 localizes at the leading edge of chemotaxing cells. Activated Rap1 regulates cell-substrate adhesion and helps establish cell polarity by locally modulating myosin2 assembly and disassembly through Ser/Thr kinase Phg2 signaling pathway (Jeon et al., 2007). It is recently shown that RapC, has high high sequence

homology with RapA, is involed in cell migration, cytokinesis, and multicellular development. Cells lacking RapC showed spread morphology and increased adhesion strength. Most *rapC* null cells were multinucleated and formed multi-tips through abnormal multicellular structures during development (Park et al., 2018). RapA and RapC have opposite functions in regulating cell spreading, adhesion, and migration (Jeon et al., 2021). When the C-terminus, the long terminal amino acid sequence of RapC, was fused to the tail region of RapA, the C-terminus reverse the functions of RapA to be similar to those of RapC (Kim et al., 2021).

Although the main functions of Rap proteins have been studied, the functions of RapB in regulating cell migration and adhesion remain unknown. Here, I investigated the functions of RapB, the protein showed the high homology with RapA which is a key regulator in cell migration and adhesion, in diverse cellular processes by examining the characteristics of cells lacking or overexpressing RapB. Furthermore, I identified the relationship between the functions of Rap proteins to regulate cell migration and adhesion using *rapB* null cells and *rapC* null cells expressing RapA, RapB, and RapC, respectively.

II. Materials and Methods

II-1. Strains and cell culture

D. discoideum wild-type Ax2 cells (DBS0237914) were obtained from the *Dictyostelium* Stock Center (DictyBase). *rapB* gene-edited cells were generated by CRISPR/Cas9 gene editing system. All the cells were cultured axenically in HL5 medium at 22 °C. The knockout strains were maintained in 10 ug/ml of blasticidin or G418.

II-2. RT-PCR

The total RNAs from wild-type cells and *rapB* null cells were extracted by using the SV Total RNA Isolation system (Promega), and the cDNAs were synthesized by reverse transcription with MMLV reverse transcriptase (Promega) using random hexamer and 500 ng of total RNAs. 1 μl of the cDNAs were used in following PCR with 35 cycles employing gene-specific primers. The universal 18S ribosomal RNA specific primers were used as an internal control (Jeon et al., 2007).

II-3. Cell adhesion assay

Cell adhesion assay was performed as described previously (Mun et al., 2014). Mid Log-phase growing cells on the plates were washed and resuspended at a density of 3.5×10^7 cells/ml in 12 mM Na/K phosphate buffer. 150 μl of the cells were placed and attached on the 6-well culture dishes. Before shaking the plates, the cells were photographed and counted for calculating the total cell number. To detach the cells from the plates, the plates were shaken at 150 rpm for

30 min, and then the attached cells were photographed and counted for the attached cell number after the medium containing detached cells was removed. Cell adhesion was presented as a percentage of attached cells compared with total cells.

II-4. Chemotaxis assay

Chemotaxis towards cAMP was examined as described previously (Jeon e*t al.,* 2007b; Mun, Lee et al., 2014). The aggregation-competent cells were prepared by pulsing with 7.5 μM cAMP at the density of 5×10^6 cells/ml in Na/K phosphate buffer for 6 h. Cell migration was analyzed using a Under Agarose Assay chamber. The images of chemotaxing cells were taken at time-lapse intervals of 1 min for 1 h using an inverted microscope (IX71; Olympus). The data were analyzed using the NIS-Elements software (Nikon) and Image J software (National Institutes of Health, NIH). Trajectory speed was used to quantify motility of the cells. The trajectory speed is the total distance moved of a cell every 1 min in a time-lapse recording. Directionality is measure of how straight the cells move. Cells moving in a straight line have a directionality of 1. It was calculated as the distance moved over the linear distance between the start and the finish.

II-5. DAPI staining

Exponentially growing cells were resuspended and placed on the coverslip in 30 mm culture plate containing 3 ml of HL5 medium. Cells washed with phosphate-buffered saline (PBS buffer, pH 7.4) and then stained with Hoechst Dye in 1 ml of mounting solution Fluoromount-G (SouthernBiotech). Epifluorescence images of random fields of view were captured by using NIS-elements software (Nikon).

II-6. Multicellular development

Multicellular development assay was performed as described previously (Jeon et al., 2009). Exponentially growing cells were harvested and washed twice with 12 mM Na/K phosphate buffer (pH 6.1) and resuspended at a density of 3.5×10^7 cells/ml. 50 μl of the cells were placed on Na/K phosphate agar plates and developed for 24 h. The developmental morphologies of the cells were photographed and examined under a phase-contrast microscope.

II-7. Statistical analysis

Statistical analysis was performed using Student's t-test (two-tailed). All data was collected from at least three independent experiments and expressed as the means ± standard deviation (SD). P value less than 0.05 was considered as statistically significant.

Table 1. Primer sequences used for RapB study

Primer name	primer	Sequence (5′ → 3′)
18s rRNA	18s rRNA - F	GTAATTCCAGCTCCAATAGC
	18s rRNA - R	GAACGGCCATGCACCAC
RapB gene edit primer	I - F	AGCAGTAATGGGCGCTGGTTCAGT
	II - R	AAACACTGAACCAGCGCCCATTAC
	III - R	AAGCTTAAAAAAAGCACCGACTCGGTGCC
RT-RCR Primer	I - F	CCCGAATTCATCAAAAGATTCAAAAGG
	II - R	CCCGGATCCGTACACTAATATAAAACC
	III - R	AGCCGGGAAACTCCTAGTGG

F - Forward, R - Reverse

III. Results

III-1. Identification of the gene encoding RapB

The Rap proteins of *Dictyostelium* consist of RapA(Rap1), RapB, and RapC. To characterize the RapB protein, I performed computer-based analysis. *Dictyostelium* RapB (DDB_G0272857) is composed of 205 amino acids (estimated molecular mass 23kDa) and contains a RAS domain at the N-terminal region (Fig. 1A). I compared RapB with other Ras proteins which function is known by multiple alignment. The RAS domain of RapB shows 86.6% sequence identities with those of *Dictyostelium* RapA(DDB_G0291237) RAS domain (Fig. 1B). I constructed phylogenetic tree with Ras proteins containing proteins. RapB showed high homology with Rap1 (Fig. 1C). Thus, these data suggest that the RapB is potential regulator of cell adhesion and cell migration.

To investigate the functions of RapB, I prepared RapB mutant strains by homologous recombination with the *rapB* gene-edited DNA construct into the *rapB* genomic DNA of Ax2 parental strains using CRISPR/Cas9 gene editing system (Fig. 2). I obtained 7 clones, which were grouped into 4 gene-edited mutants and the clones were confirmed by gene sequencing (Fig. 2A). Among them, the mutant with 144 bp insertion (*rapB* null) was used for additional confirmation through RT-PCR and subsequent experiments. *rapB* null cells inserted 144bp were confirmed by polymerase chain reaction (PCR) (Fig. 2B). PCR with a set of primers, I/II, produced band of 553 bp in wild-type cells and bands of 697 bp in *rapB* null cells, respectively (Fig. 2C, left picture). Reverse transcription (RT)-PCR using primer set I/II and cDNAs from wild-type and *rapB* null cells confirmed that the cDNAs are not contaminated by gDNAs (Fig. 2C, right picture). A band of 301 bp was observed in wild-type cells (lane 1) and a band of 445 bp was observed in *rapB* null cells (lane 2) RT-PCR using primer set I/III and cDNAs further confirmed that the insertion sequence is specific for *rapB* null cells. No band was detected in RT-

PCR experiments using cDNA from wild-type cells (lane 1), while a band of 129 bp was observed in RT-PCR experiments using cDNA from *rapB* null cells (lane 2) (Fig. 2C).

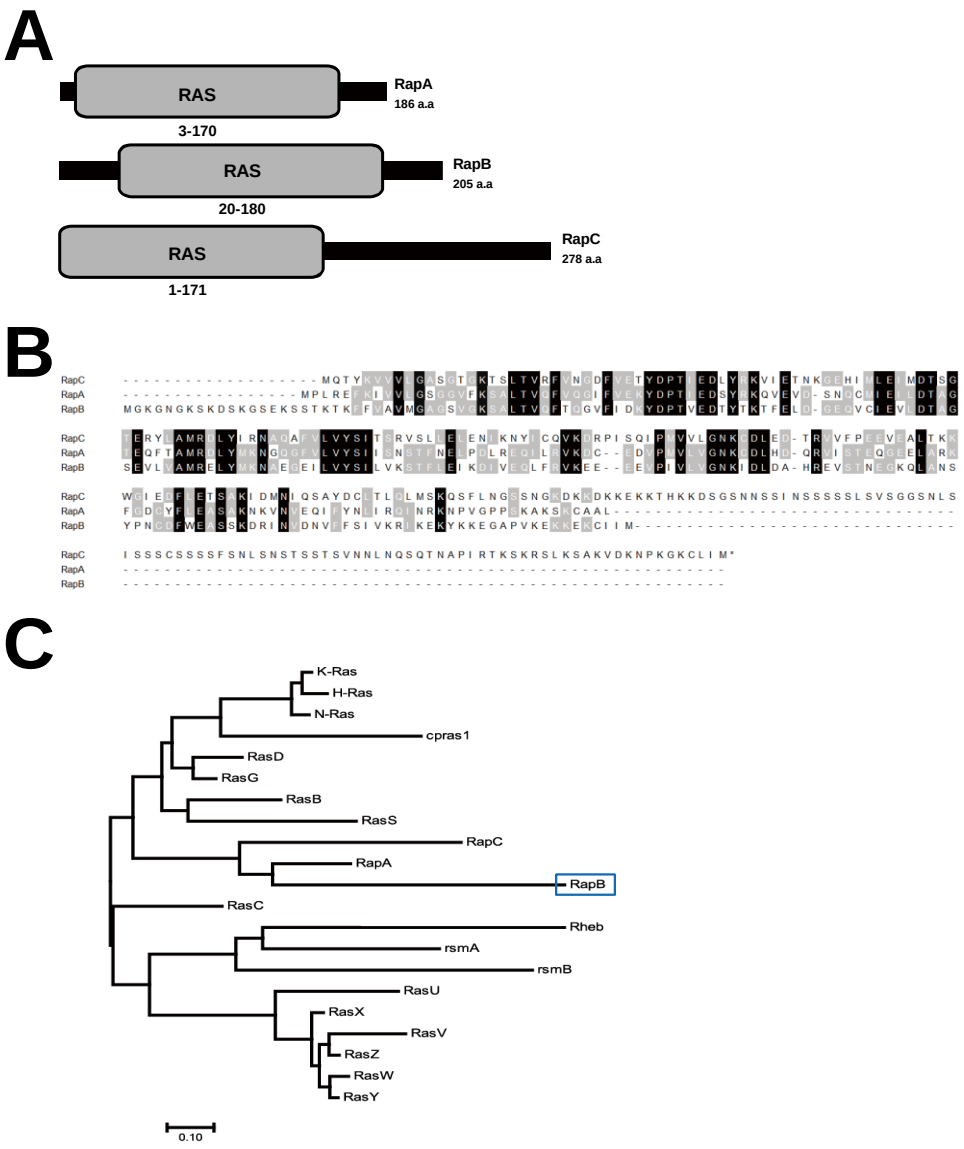

Figure 1. Domain structure and multiple alignments of RapB.

(A) Domain structure of RapB, RapA and RapC. RapB contains a Ras domain in *Dictyostelium*. (B) Multiple alignments of Ras domain in *Dictyostelium*: RapA, RapC, RapB. (C) Phylogenetic tree with Ras domains in *Dictyostelium.* The amino acid sequences of Ras are available at DictyBase.

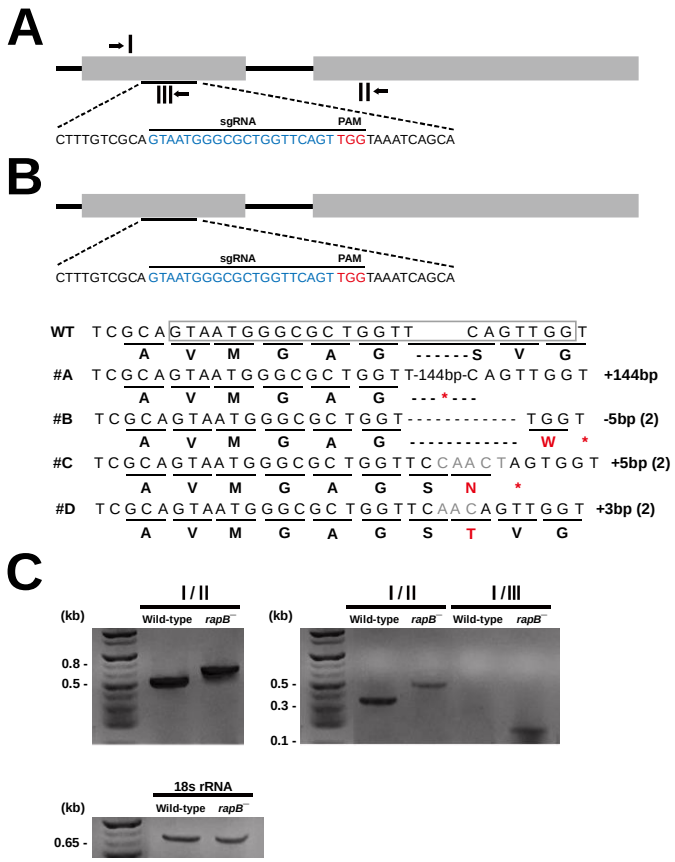

Figure 2. CRISPR/Cas9-mediated generation of *rapB* gene edited mutations in *Dictyostelium*.

(A) Schematic view of sgRNA and PAM motif targeting locus of the *rapB* genes. The blue sequence indicates the target site of the sgRNA. (B) Wild-type sequence for *rapB* and sequences derived from 4 independent positive clones by mutation detective PCR are presented. The changed amino acids and stop codon are marked in red. Numbers in parentheses indicate the number of identical clones. (C) Confirmation of *rapB* gene insertion in *rapB* null cells. Genomic DNAs from wild-type cells and *rapB* null cells were extracted and used in PCR with primer sets shown in panel A. RT-PCR using tRNAs from wild-type and *rapB* null cells and same primer set used in genomic DNAs PCR. The universal 18s rRNA specific primers were used as an internal control.

III-2. Roles of RapB in controlling cell spreading and adhesion

I first observed the phenotype of *rapB* null cells, GFP-RapB overexpressing cells (GFP-RapB cells), GFP-RapA overexpressing cells (GFP-RapA cells), and GFP-RapC overexpressing cells (GFP-RapC cells) (Fig. 3A). *rapB* null cells were smaller and more rounded than wild-type cells. In contrast, GFP-RapB cells and GFP-RapA cells were similar in cell size to wild-type cells and more flattened than *rapB* null cells. GFP-RapC cells were smaller and more rounded than wild-type cells, the same as *rapB* null cells. Measurement of cell areas using the NIS-Element software showed that *rapB* null cells and GFP-RapC cells were approximately two-thirds the size of wild-type cells (Fig. 3B). Next, I examined cell adhesion of the cells by measuring the fraction of cells that attached to the plate during agitation. Compared wild-type cells, *rapB* null cells and GFP-RapC cells showed decreased cell adhesion. GFP-RapA cells and GFP-RapB cells exhibited increased cell-substrate adhesion than wild-type cells (Fig. 3C). These results suggest that RapB is required for cell spreading and cell-substrate adhesion, similar to the functions of RapA.

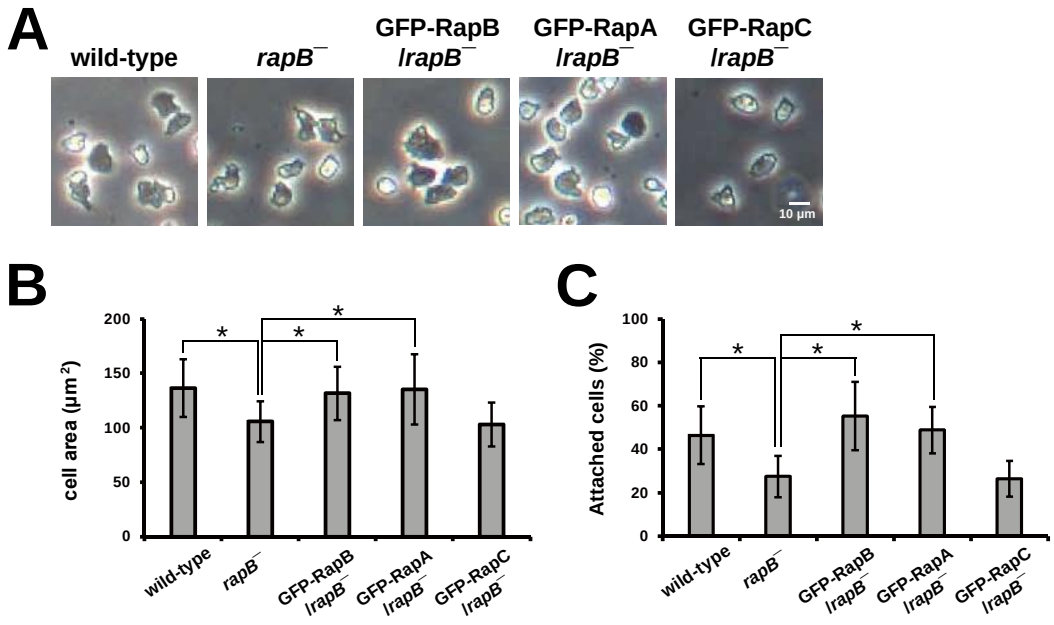

Figure 3. Cell spreading and cell adhesion of *rapB* null cells.

(A) Morphology of vegetative cells. Wild-type cells, *rapB* null cells, and GFP-RapB/*rapB*- cells, GFP-RapA/*rapB*- cells, and GFP-RapC/*rapB*- cells. Exponentially growing cells were photographed. (B) Measurement of cell area using Image J software. (C) Cell-substrate adhesion. Adhesion of the cells to the substrate was expressed as a percentage of attached cells to total cells. The values are the means ±SD of three independent experiments (*p<0.05 compared to the control by student's t-test).

III-3. Inhibition of cell migration toward chemoattractant by overexpression of RapB

RapA is known to play an important role in cell migration through cytoskeletal reorganization during chemotaxis. I expected RapB, which has high homology with RapA, to play an important role in cell migration and performed cAMP-directed cell migration experiments by under agarose chamber (Fig. 4). Aggregation-competent cells were prepared by pulsing with 7.5μM cAMP in Na/K phosphate buffer for 6 h. Wild-type cells had normal moving speed (7.5 μm/min) and directionality (0.66), which is a measure of how straight the cells move toward the chemoattractant. *rapB* null cells more polarized and elongated compared to wild-type cells. *rapB* null cells moved toward increasing cAMP concentrations with higher migration speeds (11.3 μm/min) and similar directionality (0.62) than wild-type cells. GFP-RapB cells and GFP-RapA cells showed decreased migration speed (7.39 μm/min and 7.55 μm/min, respectively) and showed normal directionality (0.68 and 0.62, respectively) compared to *rapB* null cells, which was similar to those of wild-type cells. GFP-RapC cells were not restored and exhibited migration speed (10.1 μm/min) and directionality (0.7) like *rapB* null cells. These results suggest that RapB may negatively impact on cell migration toward chemoattractant.

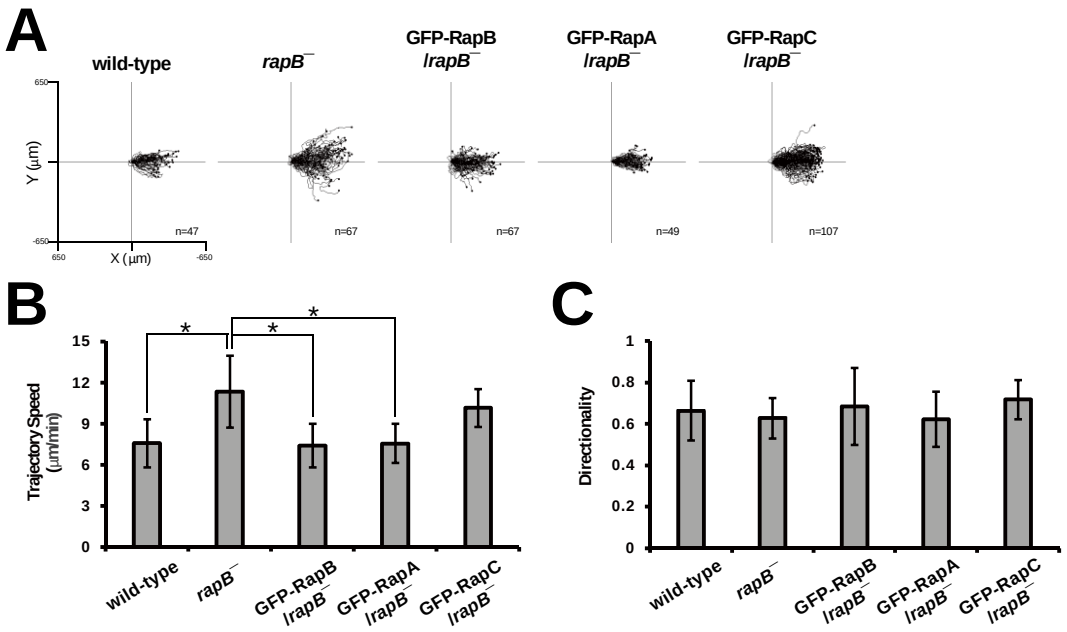

Figure 4. Chemotaxis of wild-type cells, *rapB* null cells, GFP-RapB overexpressing cells, and *rapB* null cells expressing GFP-RapA and GFP-RapC, respectively.

Aggregation-competent cells were places in Under-agarose chemotaxis chamber, and the movement of the cells up a chemoattractant, cAMP, gradient was recorded by time lapse photography for 1 h at 1 min intervals. (A) Trajectories of the chemotaxing cells. Plots show migration path of the cells with the start position of each cell centered at point 0. Cells migrate toward the increasing gradients of cAMP on the right side. Each line represents the track of a single cell chemotaxing toward 150 μM cAMP. (B) Analysis of chemotaxing cells. The recorded images were analyzed by ImageJ software. Trajectory speed indicates the speed of the cells movements along the total path. Directionality is a measure of how straight the cells move. Cells migrating in a straight line have a directionality of 1. The values are the means ±SD of two independent experiments. (Statistically different from control *p<0.05 by the student's t-test)

III-4. Complementation of *rapC* null cells by expression of RapA, RapB, and RapC

I confirmed that RapB inhibits cell migration in chemotaxis through strong cell-substrate adhesion. I further confirm that RapB and RapA have similar functions in cell migration and adhesion by showing that overexpression of RapA rescued the phenotypes of *rapB* null cells. These results indicate that RapB plays an opposite role to RapC in cell migration and adhesion. These results related to cell-substrate adhesion and cAMP-dependent cell migration were further confirmed using *rapC* null cells and overexpression RapA, RapB, and RapC cells. To further examined an opposite role of RapB to RapC, I observed the phenotype of *rapC* null cells, *rapC* null cells respectively overexpressing GFP-RapC (GFP-RapC cells), GFP-RapA (GFP-RapA cells), and GFP-RapB (GFP-RapB cells) (Fig. 5A). Cells lacking RapC were larger and more flattened than wild-type cells and GFP-RapC cells. Measurement of cell areas showed that *rapC* null cells were similar in cell size to GFP-RapA and GFP-RapB cells and were 1.7-fold larger than wild-type cells and GFP-RapC cells (Fig. 5B). In investigation of cell-substrate adhesion, *rapC* null cells showed significantly strong cell adhesion compared to wild-type cells. The strong cell adhesion of *rapC* null cells was not restored by expression of GFP-RapA or GFP-RapB (Fig. 5C). These results indicate that RapC plays an opposite role to RapA and RapB in cell spreading and cell-substrate adhesion.

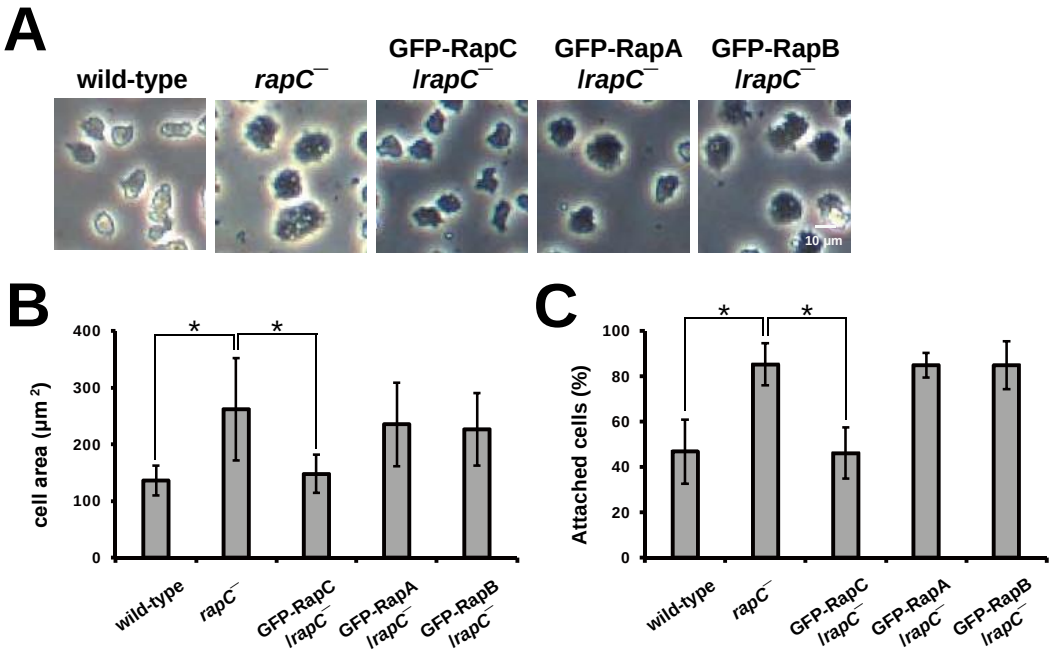

Figure 5. Cell spreading and cell adhesion of *rapC* null cells.

(A) Morphology of vegetative cells. Wild-type cells, *rapC* null cells, and GFP-RapC/*rapC*- cells, GFP-RapA/*rapC*- cells, and GFP-RapB/*rapC*- cells. Exponentially growing cells were photographed. (B) Measurement of cell area using Image J software. (C) Cell-substrate adhesion. Adhesion of the cells to the substrate was expressed as a percentage of attached cells to total cells. The values are the means ±SD of three independent experiments (*p<0.05 compared to the control by student's t-test).

Expression of RapA and RapB in *rapC* null cells did not restore the cell spreading and adhesion of *rapC* null cells. To further confirm the functional relationship in cell migration, I performed the chemotaxis assay using *rapC* null cells and overexpressing cells (Fig. 6). Upon cAMP stimulation, *rapC* null cells failed to polarize and showed non-elongated morphology compared to wild-type cells. *rapC* null cells had significantly decreased migration speeds (4.0 μm/min), which was similar to that examined in cells expressing GFP-RapA and GFP-RapB (4.1 μm/min) (Fig. 6B). The directionality was not significantly different for all those cells (Fig. 6C). These results indicate that RapB and RapA have negative role in cell migration toward chemoattractant, while RapC has an opposite function.

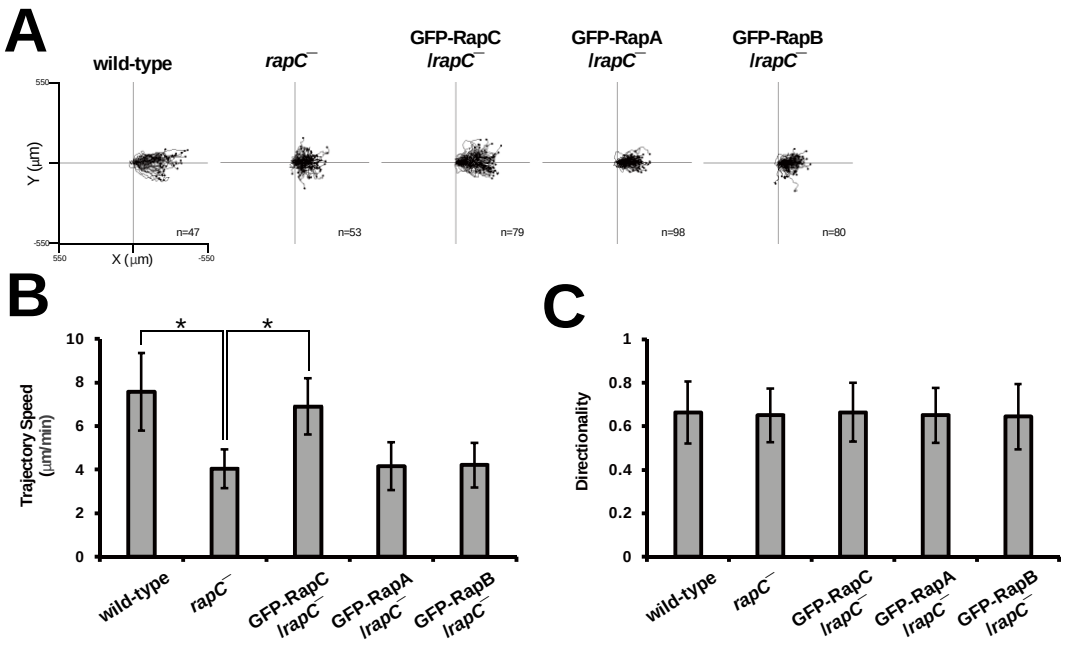

Figure 6. Chemotaxis of wild-type cells, *rapC* null cells, GFP-RapC overexpressing cells, and *rapC* null cells expressing GFP-RapA and GFP-RapB, respectively.

(A) Trajectories of the chemotaxing cells. Plots show migration path of the cells with the start position of each cell centered at point 0. Cells migrate toward the increasing gradients of cAMP on the right side. Each line represents the track of a single cell chemotaxing toward 150 μM cAMP. (B) Analysis of chemotaxing cells. The recorded images were analyzed by ImageJ software. Trajectory speed indicates the speed of the cells movements along the total path. Directionality is a measure of how straight the cells move. Cells migrating in a straight line have a directionality of 1. The values are the means ±SD of two independent experiments. (Statistically different from control *p<0.05 by the student's t-test)

III-5. Roles of RapB in cytokinesis and development

Examination of the number of nuclei with Hoechst dye to investigate the role of RapB in cytokinesis (Fig. 7). Majority of wild-type cells and *rapB*_null cells, and *rapB* null cells expressing GFP-RapA, GFP-RapB, and GFP-RapC contained on nucleus. These results suggest that RapB is not involved in cytokinesis.

Upon starvation, *Dictyostelium* cells release cAMP, causing surrounding cells to migrate toward the cAMP source and initiate their molecular development process (Chisholm and Firtel, 2004). *rapB* null cells showed increased migration speed toward cAMP compared to wild-type cells. To examine the possible in vivo roles of RapB in development, I performed development assay (Fig. 8). Wild-type cells, *rapB* null cells, and *rapB* null cells expressing GFP-RapA, GFP-RapB, and GFP-RapC, respectively, developed normally, forming mounds at 8 h, multicellular slug at 14 h, and finally single fruiting bodies at 24 h. (Fig. 8A). In contrast, *rapC*_null failed to form a slug at 14 h and to form fruiting bodies and finally formed multi-tips from a single mound. The developmental phenotypes of *rapC* null cells were not rescued by expression of GFP-RapA and GFP-RapB but rescued by expression of GFP-RapC (Fig. 8B). These results suggest that RapB is not required for proper development and cannot replace the developmentally specific functions of RapC.

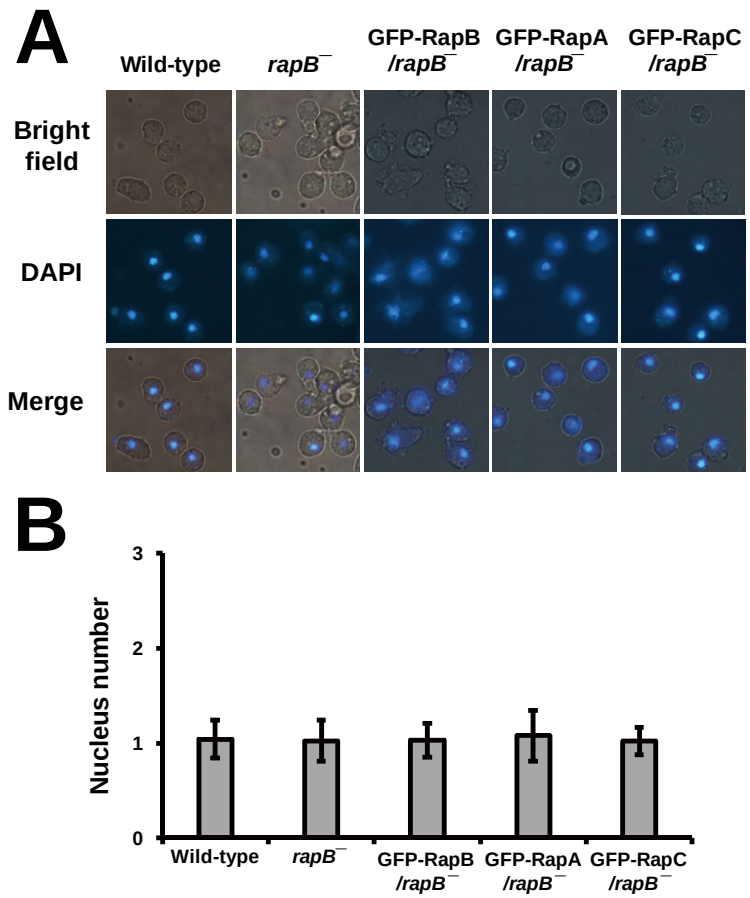

Figure 7. The cytokinesis of the cells.

(A) Morphology of the cells. Vegetatively grown wild-type cells. DAPI images of the cells. Corresponding phase-contrast and merged images are shown on the top and bottom panels, respectively. (B) Quantitative of the number of nuclei in the cells. Mean values of the number of nuclei were graphed. Error bars represent ±SD of three independent experiments. Statistically different from control at *$p<0.05$ by the student's t-test.

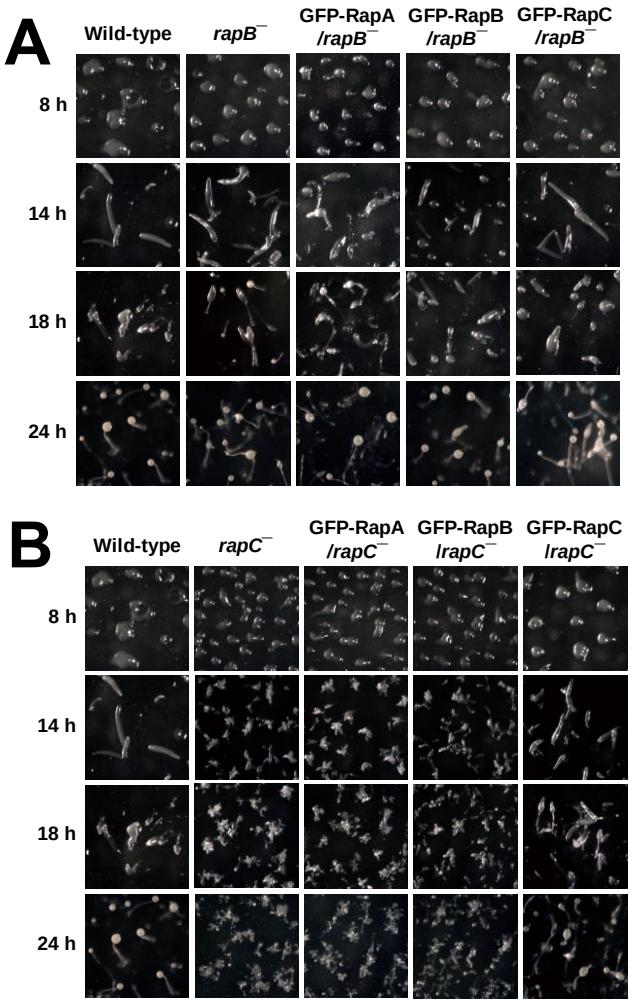

Figure 8. Multicellular development of the cells.

Development of non-nutrient agar plate. Exponentially growing cells were washed and plated on non-nutrient agar plates. Photographs were taken at the indicated times after plating. Representative developmental images of the cells at 8h (aggregation stage), at 14h (elongation stage), at 18h and 24h (fruiting body formation stage) are shown. (A) Development of *rapB* null cells (B) Development of *rapC* null cells.

IV. Discussion

The small GTPase Rap1 is involved in the control of diverse cellular processes, including integrin-mediated cell adhesion, cadherin-based cell-cell adhesion, cell polarity, and cell migration. Identified RapB is Ras subfamily proteins showing the high homology with Rap1, which is a key regulator in cell adhesion and cell migration (Lee and Jeon, 2012). Of the three Rap proteins, RapB has not yet been shown to regulate cell adhesion and migration. In the study, I investigated functions of RapB in regulating cell adhesion and cell migration and examined the functional relationship between RapB, RapA and RapC proteins.

rapB null cells showed decreased cell size and cell-substrate adhesion. The cells overexpressing GFP-RapB showed rescued cell size and cell-substrate adhesion similar to wild-type cells. When deprived of nutrients, *rapB* null cells elevated their chemotactic abilities to move toward increasing concentrations of the chemoattractant by weak cell adhesion compared to wild-type cells. These results demonstrate that RapB plays a positive role for cell spreading and cell-substrate adhesion and plays a negative role for cell migration.

As these phenotypes of RapB are similar to those of RapA and opposite to those of RapC, I overexpressed GFP-RapA and GFP-RapC in *rapB* null cells to examine if the phenotypes of *rapB* null cells were restored. *rapB* null cells expressing RapA restored cell size and cell adhesion, and migration speed toward to chemoattractants similar to GFP-RapB cells. However, *rapB* null cells expressing RapC did not restore these phenotypes. To further confirm this, I overexpressed GFP-RapA and GFP-RapB in *rapC* null cells and observed the phenotypes. *rapC* null cells expressing RapA or RapB did not reduce the cell spreading and strong adhesion of *rapC* null cells and showed decreased migration speed to chemoattractants compared to GFP-RapC cells. These results indicate that the functions of RapB in regulating cell spreading, adhesion, and cell migration is similar to RapA and opposite to RapC.

In *Dictyostelium* cells, rapid cell migration to chemoattractants induces fast cellular aggregation and early formation of multicellular organisms during development. However, *rapB*

null cells did not show significant temporal or morphological differences than wild-type cells and GFP-RapB cells. To supplement this, when deprived of nutrients, dominantly negative form of GFP-RapB cells (GFP-RapB^{S36N} cells) showed faster aggregation and early formation of multicellular mold than wild-type cells. In contrast, constitutively active form of GFP-RapB cells (GFP-RapB ^{G31V} cells) showed slow cell migration and developed than wild-type cells (unpublished data). These results suggest that RapB required for proper cell migration and development. Furthermore, overexpression of GFP-RapA and GFP-RapB in *rapC* null cells failed to restore the unique developmental phenotype of *rapC* null cells and resulted in the formation of specific multi-tips during development. These results indicate the unique function of RapC in cell development, which does not involve RapA and RapB.

There is a putative factor as to why RapA and RapB have similar functions in regulating cell adhesion and migration, but RapC does not. RapC has an additional amino acid sequence in tail region, the C-terminus, that is longer than the sequence of RapA and RapB. This C-terminal region is essential for RapC, and when fused with tail region of RapA, it was able to reverse the function of RapA and becomes similar to that of RapC (Kim *et al.*, 2021). It is speculated that the C-terminus of RapC is the main factor that causes RapC to function in opposition to RapA and RapB. Whether the C-terminus can also reverse the functions of RapB is under investigation, and the mechanism by which the C-terminus reverses the functions of RapA is still unknown and requires further study.

PART II. Role of NHE1 in cell migration and phagocytosis in *Dictyostelium*

I. Introduction

Intercellular pH homeostasis is important for the maintenance of physiological processes in the human body, including cell proliferation and apoptosis, and assembly and depolymerization of the cytoskeleton. Disruption of intracellular and extracellular pH balance is an important factor in tumorigenesis and continued tumor development (Reshkin et al., 2000). Pseudopodia, which are composed primarily of actin and assemble microfilament networks that protrude into the extracellular matrix (ECM) and induce cytoskeleton formation, are the driving force of tumor cell migration and invasion (Hu et al., 2021). Therefore, the acidic extracellular microenvironment of tumor cell is an important factor to malignant transformation (Brisson et al., 2012). The formation of the extracellular acid-base environment mainly depends on the efflux of excess intracellular hydrogen ions by intracellular and extracellular pH regulators such as the Na^+/H^+ exchanger (NHE) (Hu *et al.*, 2021). The NHE family of membrane integral proteins is widely expressed in eukaryotic cells and regulates intracellular and extracellular pH balance primarily through the exchange of intracellular H^+ with extracellular Na^+ (Dibrov and Fliegel, 1998).

The predominant polymerization of F-actin at the leading edge for propulsion is necessary for chemotaxis of amoeboid cells such as *Dictyostelium* (Parent, 2004). *Dictyostelium* is an important model to study chemotactic migration because the mechanics and regulation of F-actin dynamics are similar to those in migrating mammalian cells (Sasaki and Firtel, 2006). In *Dictyostelium discoideum*, intracellular pH is important for directed cell migration. Increased

intracellular H+ efflux is an evolutionarily conserved mechanism required for rapid assembly of cytoskeletal filaments and for morphological polarity during cell motility. *Dictyostelium* Na-H exchanger is predominantly localized at the leading edge of chemotaxing cells, and reported that is necessary for cell polarity and chemotaxis in response to cAMP-induced increased in intracellular pH (Patel and Barber, 2005).

Cell migration, such as chemotaxis, can be induced by a variety of chemical and physical cues. Directed migration in an electric field (EF), called galvanotaxis or electrotaxis, occurs in many types of cells, and may play an important role in would healing and development (Gao et al., 2015). Although the mechanisms of chemotaxis have been well studied, the mechanisms by which the cells sense the weak direct current (DC) EFs has remained unknown. It is not clear, however, it has been shown to be likely that a response of cells to a large voltage gradient is due to the difference in the membrane potential that is set up by the field (Robinson, 1985). One of the immediate effects felts by a cell upon exposure to an EF is a change in the cell membrane potentials (*Vm*) (Gao et al., 2011). In an EF, the cathodal side of plasma membrane depolarizes whereas the membrane facing the anode hyperpolarizes (Mycielska and Djamgoz, 2004). These transmembrane potential or ionic current changes may play a role in signal transduction and differentiation in the *Dictyostelium* (van Duijn and Vogelzang, 1989).

NHE1, a Na-H antiporter, has been primarily studied for its functions in chemotaxis in *Dictyostelium*. To determine how the transmembrane exchanger that transports sodium and hydrogen, which are involved in the depolarization of the cells, affect the electrotaxis, *Dictyostelium* cells were used to confirm the phenotypes with *nhe1* null cells. This will provide a basis for studies of the role of membrane potential in the regulation of intracellular and extracellular sodium-hydrogen. I further confirmed that the possible role of NHE1 in phagocytosis by determining the responsiveness of *nhe1* null cells to chemoattractants based on cell state.

II. Materials and Methods

II-1. Strains and cell culture

Dictyostelium discoideum cells were obtained from the *Dictyostelium* Stock Center, wild-type Ax2(DBS0350762, Gerry Weeks lab strain) and *nhe1* null cells, and NHE1 cells. All cells were cultured axenically in HL5 medium at 22°C. Nhe1 com cells were maintained in 10ug/ml G418.

II-2. Cell adhesion assay

Mid Log-phase growing cells on the plates were washed and resuspended at a density of 3.5 × 10^7 cells/ml in 12 mM Na/K phosphate buffer. 150 μl of the cells were placed and attached on the 6-well culture dishes. Before shaking the plates, the cells were photographed and counted for calculating the total cell number. To detach the cells from the plates, the plates were shaken at 150 rpm for 30 min, and then the attached cells were photographed and counted for the attached cell number after the medium containing detached cells was removed. Cell adhesion was presented as a percentage of attached cells compared with total cells.

II-3. Electrotaxis assay

Electrotaxis using vegetative cells starved for 3 h was performed as described previously (Jeon et al., 2019). Fully grown cells on 24-well plates were washed three times and starved for 3 h in development buffer (DB; 5 mM Na2HPO4, 5 mM KH2PO4, 2mM MgCl2 and 1mM CaCl2) and then used to electrotaxis assay. For experiments with aggregation-competent cells,

exponentially growing cells were washed twice and resuspended at a density of 5×10^6 cells/ml in DB buffer. The cells were pulsed with 30 nM cAMP every 6 min for 6 h. All procedures were performed at room temperature (~22°C). The prepared cells were seeded in an electrotactic chamber for 30 min and the unattached cells were washed off using DB buffer. A roof of cover glass was placed on the cells within a trough and sealed with silicone grease. Each chamber was then filled with sufficient DB buffer. EF was applied at the indicated field strength through agar salt bridges. Cell migration was recorded at intervals of 1 min for 1 h using an inverted microscope (IX71; Olympus) with a camera (DS-Fil; Nikon) controlled by the NIS-Elements software (Nikon).

Time-lapse recordings of cell migration were analyzed using ImageJ (National Institutes of Health). Directedness quantifies how directionally cells migrate in response to an EF. The directedness of the movement of the cells was measured as cosine θ, where θ is the angle between the direction of the field and a straight line connecting the start and end positions of the cell. Trajectory speed was assessed by dividing the total distance travelled by the cell by time. All data were obtained and analyzed from at least three independent experiments.

II-4. Chemotaxis assay

The aggregation-competent cells were prepared by pulsing with 7.5 μM cAMP at the density of 5×10^6 cells/ml in Na/K phosphate buffer for 6 h. Cell migration was analyzed using a Under Agarose Assay chamber. The images of chemotaxing cells were taken at time-lapse intervals of 1 min for 1 h using an inverted microscope (IX71; Olympus). The data were analyzed using the NIS-Elements software (Nikon) and Image J software (National Institutes of Health, NIH). Trajectory speed was used to quantify motility of the cells. The trajectory speed is the total distance moved of a cell every 1 min in a time-lapse recording. Directionality is measure of how

straight the cells move. Cells moving in a straight line have a directionality of 1. It was calculated as the distance moved over the linear distance between the start and the finish.

II-5. Multicellular development

Exponentially growing cells were harvested and washed twice with 12 mM Na/K phosphate buffer (pH 6.1) and resuspended at a density of 3.5×10^7 cells/ml. 50 µl of the cells were placed on Na/K phosphate agar plates and developed for 24 h. The developmental morphologies of the cells were photographed and examined under a phase-contrast microscope.

II-6. Measurement of cytosolic calcium

The cytosolic calcium level of cells was measured by the fluorescence image using cytosolic calcium marker GCaMP3. Vegetative cells and aggregation competent cells were attached to the plate for 30 min. The cells were uniformly stimulated by quickly treatment 220 µl chemoattractant using pipetting into the plate containing cells. The fluorescence images were taken at time-lapse intervals of 2 sec for 1 min by using NIS-elements software (Nikon) and ImageJ software (National Institutes of Health, NIH). The intensity of the fluorescence in the cytosol was measured, and the relative of GCaMP3 was calculated by dividing the intensity before stimulation (E_o) with the intensity at each time point (E_t).

II-7. Phagocytosis assay

Phagocytosis was performed based on a published protocol (Pontel et al., 2016). Exponentially growing bacteria (*K. aerogenes* cells) in SM media were placed on the SM

plated and then 3.5×10^4 cells were seeded. Photographs were analyzed using Image J software (National Institutes of Health)

II-8. Statistical analysis

Statistical analysis was performed using Student's t-test (two-tailed). All data was collected from at least three independent experiments and expressed as the means ± standard deviation (SD). P value less than 0.05 was considered as statistically significant.

III. Results

III.1. characterization of the gene encoding NHE1

To characterize the NHE1 protein, I performed computer-based analysis. *Dictyostelium* NHE1 (DDB_G0275711) is composed of 674 amino acids (estimated molecular mass 75kDa) and contains a Na-H exchanger domain at the N-terminal region (Fig. 9A). Compared the *D.d*NHE1, NHE1 of *H.sapiens* has a N-H exchanger domain and extra TM domain at N-terminal region and NEXCaMBD at C-terminal region. Multiple alignments using the amino-acid sequences of the full-length NHE1 family proteins showed that they have Na-H exchanger domain. Phylogenetic analysis showed that *D.discoideum* NHE1 had the high homology with *D.melanogaster* NHE1 (62.5%) and *H.sapiens* NHE1 (53.3%) (Fig. 9B).

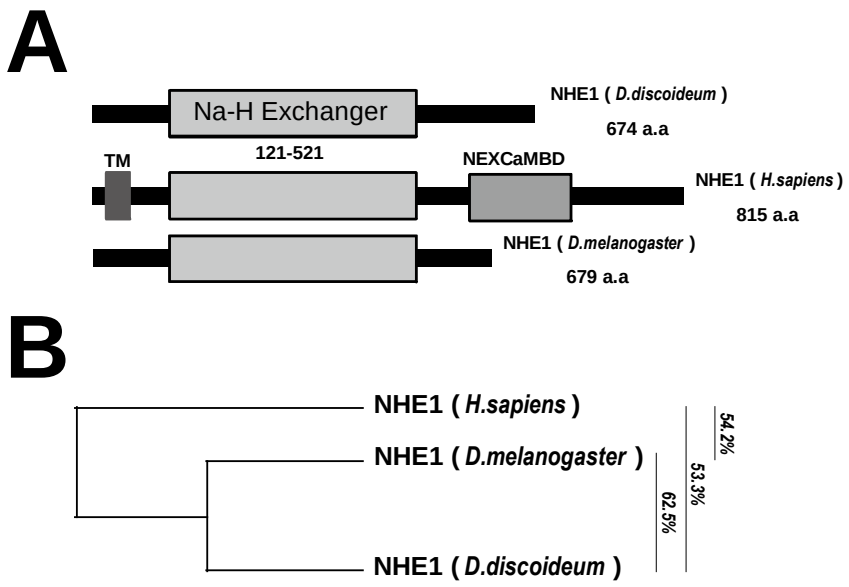

Figure 9. Domain structure and phylogenetic tree of NHE1.

(A) Domain structures of *Dictyostelium* NHE1 and NHE1 family. (B) phylogenetic tree of Nhe1 family. The full sequence amino acid of NHE1 and NHE1 family were aligned by MEGAX. NHE1_*D.discoideum* (DDB_G0275711); NHE1_*H.sapiens*; NHE1_*D.melanogaster*.

III.2. Role of NHE1 in cell spreading and adhesion

To investigate the roles of NHE1 in the regulation of cell spreading and cell adhesion, I observed the morphology and cell adhesion of *nhe1* null cells and NHE1 overexpressing cells (NHE1 cells) (Fig. 10A). *nhe1* null cells were smaller and more rounded than wild-type cell. Measurement of cell areas using the NIS-Elements software showed that *nhe1* null cells were half of wild-type cells and NHE1 cells had similar size compared to wild-type cells (Fig. 10B). In examination of cell adhesion by measuring the fraction of cells that attached to the plate during agitation, *nhe1* null cells showed decreased cell adhesion. NHE1 cells showed a similar cell-substrate adhesion with wild-type cells (Fig. 10C). These results indicate that NHE1 is required for proper cell spreading and cell-substrate adhesion.

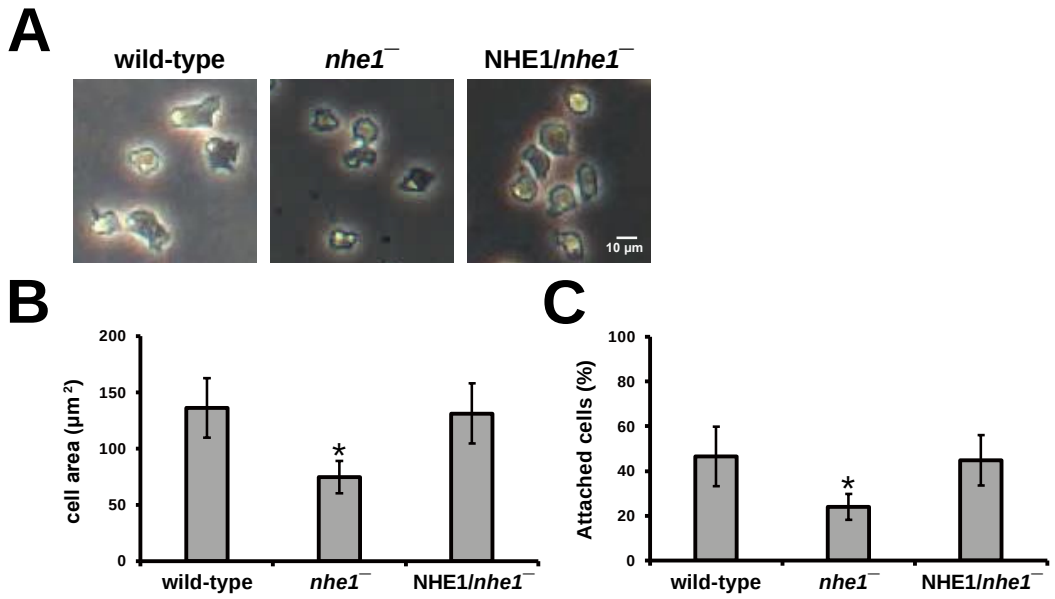

Figure 10. Cell spreading and cell adhesion of *nhe1* null cells.

(A) Morphology of vegetative cells. Wild-type cells, *nhe1* null cells, and NHE1 cells. Exponentially growing cells were photographed. (B) Measurement of cell area using Image J software. (C) Cell-substrate adhesion. Adhesion of the cells to the substrate was expressed as a percentage of attached cells to total cells. The values are the means ±SD of three independent experiments (*p<0.05 compared to the control by student's t-test).

III.3. Promotion of cell migration by NHE1 expression in vegetative state

To determine whether NHE1, a sodium-hydrogen cation antiporter, functions in response to electrical stimulation, I performed electrotaxis using vegetative cells and aggregation-competent cells (Fig. 13). Cell migration in the electrotaxis chamber was recorded for 60 min at 1 min intervals. 15V/cm of electric field was applied for 30 min (EF; 10-40 min for 60min). The electric field was turned off at the first 10 min (Before) and the last 20 min (After) for 60 min recording to check random motility of the cells in absence of electric field.

In vegetative state, upon exposure to EF, wild-type cells and NHE1 cells showed the similar migration pattern of an immediate response to electric stimulation. Migration speed of cells gradually increased to the maximum level within 10 min and remained at the maximum level through the duration of decreased back to the basal level (Fig. 11A). However, *nhe1* null cells showed a significant difference in the migration speed and directedness compared to wild-type cells. Although wild-type cells and NHE1 cells increase their migration speed upon EF (7 μm/min), *nhe1* null cells did not increase their migration speed upon EF (5 μm/min) (Fig. 13B). Upon EF stimulation, wild-type cells and NHE1 cells increased directedness toward electric stimulation (0.7 and 0.8). In contrast, the directedness of *nhe1* null cells increased slightly, but they migrated almost randomly, and had low directedness (0.2) (Fig. 11B).

In electrotaxis using aggregation-competent cells, *nhe1* null cells showed similar level of motility to wild-type cells and NHE1 cells. Wild-type cells, *nhe1* null cells and NHE1 cells showed directed migration response to electric stimulus when the EF was turned on and migrated randomly when the EF was turned off (Fig. 11C). Basically, wild-type cells and NHE1 cells increased their migration speed upon EF (10.1 μm/min and 9.8 μm/min), and *nhe1* null cells did not increase migration speed upon EF (8.2 μm/min), however, there was no significant difference in migration speed between wild-type cells, *nhe1* null cells and NHE1 cells. In addition, unlike the results using vegetative cells, aggregation-competent *nhe1* null cells showed a high

directedness to EF similar to wild-type cells and NHE1 cells (0.88) (Fig. 11D). These results suggest that NHE1 is required for cell migration and orientation in response to electric stimulation in vegetative state.

Although the previous experiments used aggregation-competent cells to investigate the functions of NHE1 in chemotaxis, I confirmed that NHE1 is required to electrotaxis in vegetative state. To determine the functions of NHE1 in chemotaxis in vegetative state, I performed chemotaxis according to the developmental state of the cells using vegetative and aggregation-competent cells as in electrotaxis (Fig. 12).

In vegetative state, compared to wild-type cells and NHE1 cells, which have high migration speed in response to chemoattractants (9.2 μm/min), *nhe1* null cells had a slower migration speed (6.2 μm/min). *nhe1* null cells also had lower directionality toward chemoattractants compared to wild-type cells and NHE1 cells and moved almost randomly (Fig. 12C). These results suggest that NHE1 is also required for chemotaxis in vegetative cells, in addition to the previous studies that NHE1 is required for chemotaxis in aggregation-competent cells.

During development, as shown in Figure 13, *nhe1* null cells delayed cell aggregation and failed to form mounds properly at ~8h with temporal and morphological difference to those of wild-type cells. Also, *nhe1* null cells formed fruiting bodies at 24h identical to wild-type cells, however, the formed slugs and fruiting bodies were smaller than wild-type cells. These results suggest that NHE1 is required for proper development.

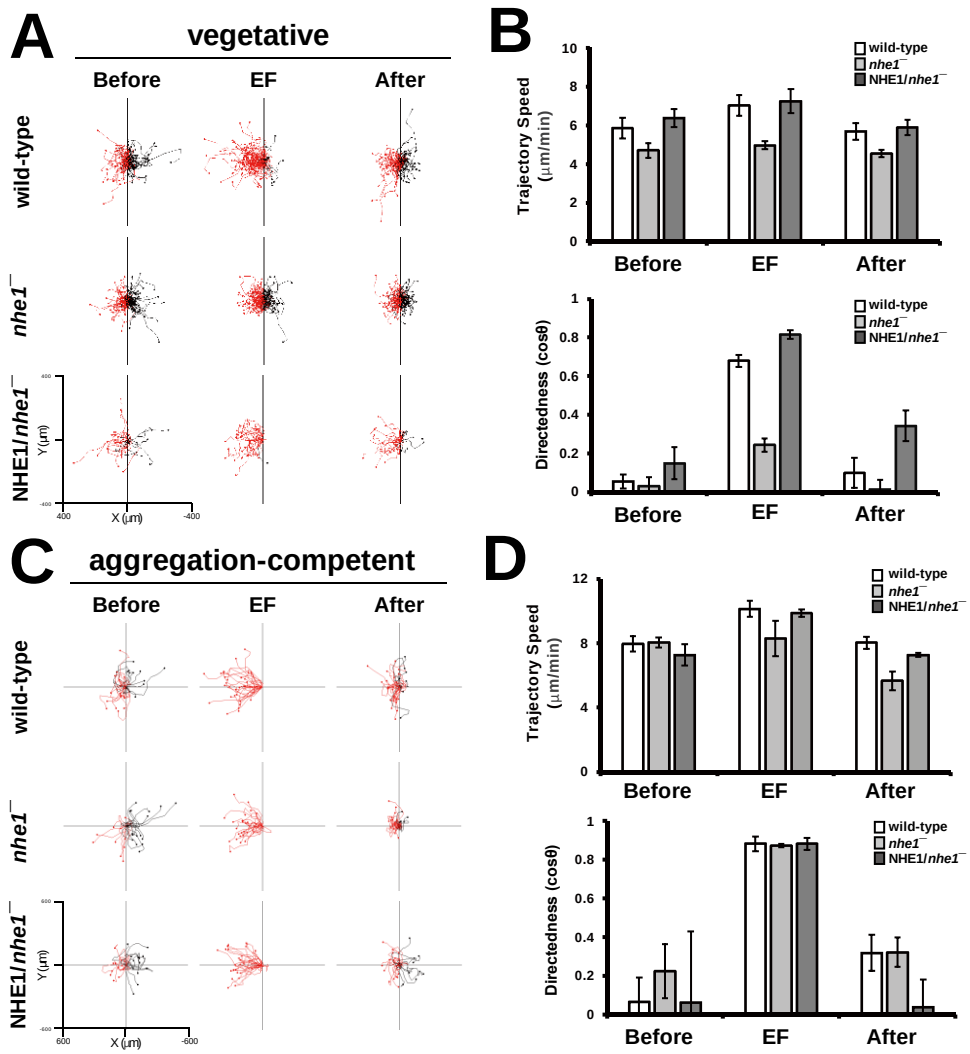

Figure 11. Electrotaxis of *nhe1* null cells according to developmental state.

(A) Trajectories of wild-type cells and *nhe1* null cells, and NHE1 cells in vegetative state (Before 1-10 min, EF 31-40 min, After 41-50 min). (B) Quantitative analysis of the trajectory speed and directedness of *nhe1* null cells in vegetative state. (C) Trajectories of the cells in aggregation-competent state. (D) Quantitative analysis of the trajectory speed and directedness of the cells in aggregation-competent state. The values are the means ±SEM of three independent experiments.

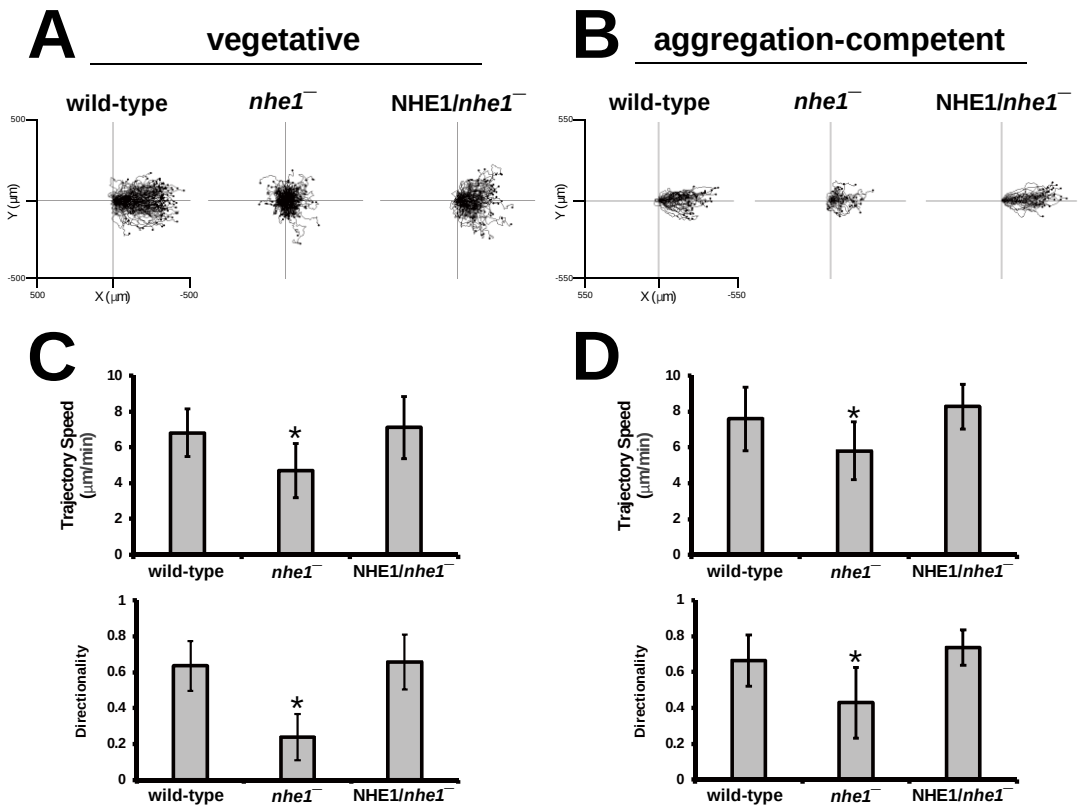

Figure 12. Chemotaxis of wild-type cells, *nhe1* null cells, and NHE1 cells.

(A) Trajectories of the chemotaxing cells in vegetative state. Plots show migration path of the cells with the start position of each cell centered at point 0. Cells migrate toward the increasing gradients of cAMP on the right side. Each line represents the track of a single cell chemotaxing toward 150 μM cAMP. (B) Trajectories of the chemotaxing cells in aggregation-competent state. (C) Analysis of chemotaxing cells in vegetative state. (D) Analysis of chemotaxing cells in aggregation-competent state. The recorded images were analyzed by ImageJ software. Trajectory speed indicates the speed of the cells movements along the total path. Directionality is a measure of how straight the cells move. Cells migrating in a straight line have a directionality of 1. The values are the means ±SD of three independent experiments. (Statistically different from control *p<0.05 by the student's t-test)

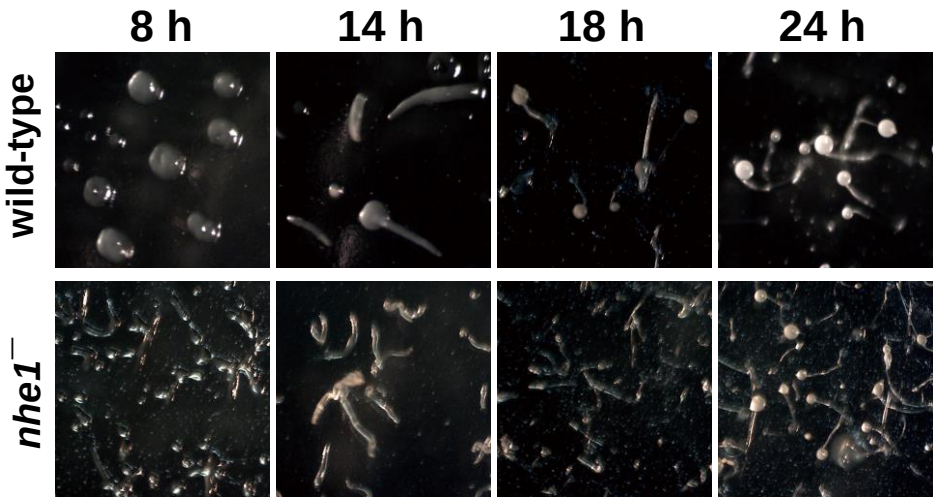

Figure 13. Development of the cells.

Development of non-nutrient agar plate. Exponentially growing cells were washed and plated on non-nutrient agar plates. Photographs were taken at the indicated times after plating. Representative developmental images of the cells at 8h (aggregation stage), at 14h (elongation stage), at 18h and 24h (fruiting body formation stage) are shown. Development of wild-type cells, *nhe1* null cells, and NHE1 cells.

III.4. Roles of NHE1 in phagocytosis

In chemotaxis, I confirmed that *nhe1* null cells decreased migration speed and directionality toward chemoattractants. To further confirm the responsiveness of NHE1 to chemical stimulation, the cytosolic calcium marker GCaMP3 was expressed in wild-type cells and *nhe1* null cells to examine the activity to chemoattractants based on developmental state of the cells. Using vegetative cells, when wild-type cells and *nhe1* null cells were treated with folic acid at 4s, wild-type cells showed increasing of fluorescence immediately upon stimulation, reaching a peak at 20s. In contrast, *nhe1* null cells did not respond immediately upon stimulation and cytosolic fluorescence increased slowly, reaching a small peak at 40s (Fig. 14B). When aggregation-competent wild-type cells and *nhe1* null cells were treated with cAMP at 4s, wild-type cells and *nhe1* null cells similarly increased upon stimulation starting at 10s, reaching a peak at 20s and decreasing thereafter (Fig. 14D).

Dictyostelium cells feeds on bacteria and they chase bacteria by chemotaxing towards folic acid, which is secreted by the bacteria (Kortholt and van Haastert, 2008). Phagocytosis is actin-dependent processes mainly performed by cells like neutrophils. Phagocytosis consists of a number of stages including attachment of particles to cell surface receptors, engulfment of particle dependent on actin polymerization, and formation of phago-lysosomes (Cardelli, 2001).

NHE1 protein is known to be involved in F-actin polymerization by regulation of intracellular pH. Based on the low responsiveness of *nhe1* null cells to folic acid, wild-type cells and *nhe1* null cells were plated on the plates which *K.aerogenes* bacteria were placed to investigate the functions of NHE1 in the phagocytosis. 3 days after plating, the colony size of *nhe1* null cells were found to be smaller than wild-type cells (Fig. 15B). The growth rate of *nhe1* null cells also much lower than wild-type cells (Fig. 15C). These results indicate that NHE1 is required for phagocytosis.

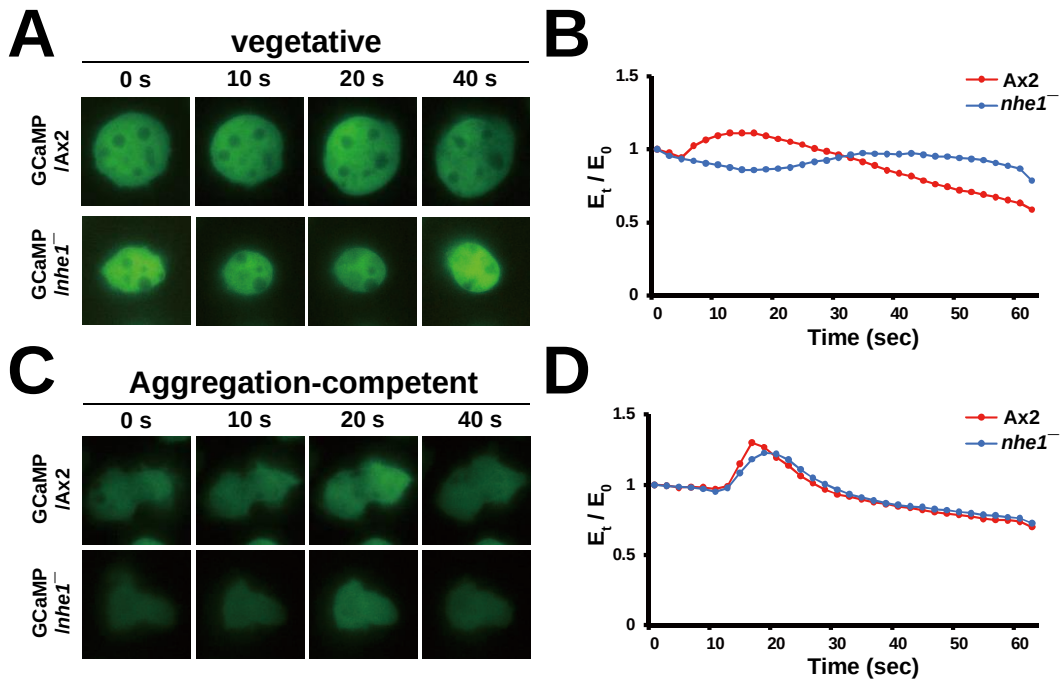

Figure 14. Measurement of the cytosolic calcium level by chemoattractant stimulation.

(A) Fluorescence of GCaMP proteins of wild-type cells and *nhe1* null cells after folic acid stimulation in vegetative state. (B) Quantification of the cytoplasmic fluorescence intensity of vegetative cells upon folic acid stimulation. (C) Fluorescence of GCaMP proteins of wild-type cells and *nhe1*- cells after cAMP stimulation in aggregation-competent state. (D) Quantification of the cytoplasmic fluorescence intensity of aggregation-competent cells upon cAMP stimulation.

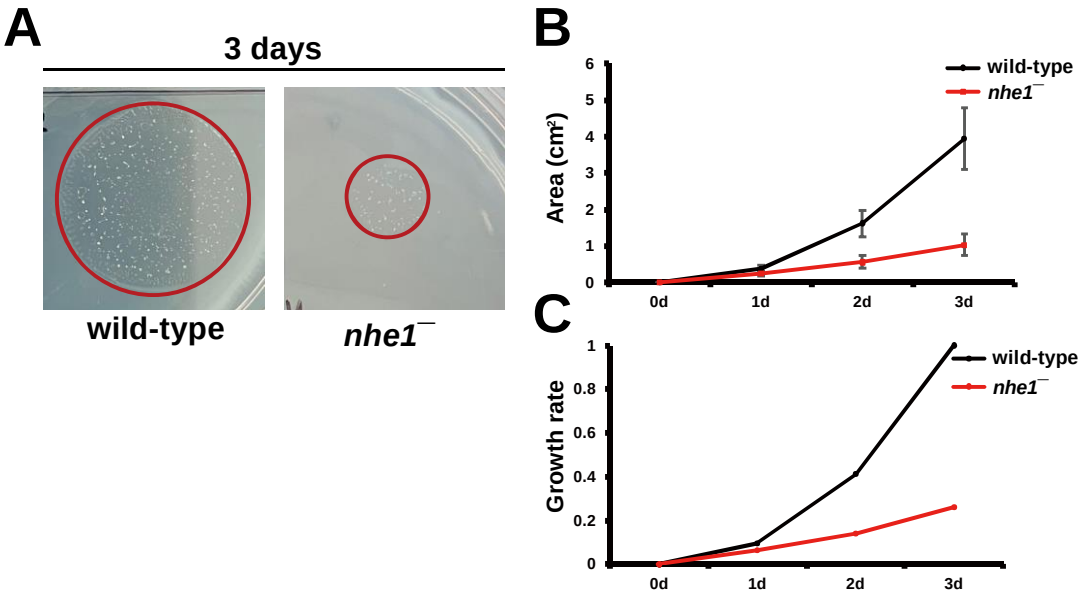

Figure 15. phagocytosis of wild-type cells and *nhe1* null cells.

(A) Wild-type cells and *nhe1* null cells were plated on agar plates coated with *K.aerogenes*. Photographs were taken at the 3 days after plating. (B) Measurement of colony diameter. The diameters of the colonies were measured using Image J software. (C) Growth rate of the colonies.

IV. Discussion

In *Dictyostelium*, cAMP induces an increase in pH_i that is essential for directional movement(Van Duijn and Inouye, 1991). A *Dictyostelium* Na-H exchanger, NHE1, is the predominant regulator of increased pH^i in response to cAMP and localizes to the leading edge of polarized cells and is necessary for intracellular pH homeostasis and for efficient chemotaxis. Loss of NHE1 induced the cells cannot attain a polarized morphology, but instead extend mis-localized pseudopodia around the cell resulting exhibition decreased migration speed(Patel and Barber, 2005). NHE1 has been mainly studied for its functions in chemotaxis, and I focused on electrotaxis to examine the functions of NHE1, a cation exchanger, regulating cell migration in response to electrical stimulation.

nhe1 null cells showed decreased cell size and cell-substrate adhesion. When cell adhesion is reduced, cell migration speed usually improves, in contrast, *nhe1* null cells did not performed F-actin polymerization properly, resulting in decreased migration speed. Examination of cell migration in response to electrical stimulation revealed that *nhe1* null cells showed decreased migration speed with very poor directionality compared to wild-type cells and NHE1 cells in vegetative state. However, when electrically stimulation using aggregation-competent cells, *nhe1* null cells exhibit migration speed similar to wild-type cells and high directionality to EF. These results indicate an important role of NHE1 in electrotaxis in vegetative state.

Identification of defect in electrotaxis, I next examined whether NHE1 also affects chemotaxis in vegetative state and found that *nhe1* null cells migrate slower and showed decreased directionality toward chemoattractants in vegetative state. These phenotypes of *nhe1* null cells were restored by overexpression of NHE1, resulting in migration speed and directionality similar to wild-type cells. These results suggest that NHE1 plays an important role in cell migration in response to chemical or electrical stimuli, not only in the aggregation-competent state, but also in cells in the vegetative state.

I further examined how loss of NHE1 affects responsiveness to extracellular chemoattractants using the cytosolic calcium marker GCaMP3 and found that when vegetative cells were treated with the folic acid, *nhe1* null cells had less response and slower increase in fluorescence compared to wild-type cells. Based on the low responsiveness of *nhe1* null cells to chemoattractants secreted by bacteria, I investigated additional possible role of NHE1 in phagocytosis. *nhe1* null cells were defective in forming colonies, resulting in poor colony growth compared to wild-type cells, which formed larger colonies over time. These results suggest additional functions of NHE1 in cell migration as well as phagocytosis.

Phagocytosis requires actin cytoskeleton remodeling to produce distinct F-actin-rich membrane structures (Rougerie et al., 2013). Cytosolic Ca^{2+}, a secondary messenger during phagocytosis, is a ubiquitous intracellular signal that plays pivotal role in several signal transduction pathways. Cytosolic Ca2+ regulates a diversity of cellular activities, including proliferation and differentiation, and cell death (Berridge et al., 2000). Cytosolic Ca2+ is speculated to regulate the depolymerization of actin during phagocytosis, however, the mechanism remains unknown. Loss of NHE1, which regulates the polymerization of the cytoskeleton through intracellular pH regulation, inhibits the polymerization of F-actin. Inhibited F-actin polymerization results in defective phagocytosis and is speculated to reduce the cytosolic calcium elevation in response to folic acid, a chemoattractant secreted by bacteria, in *nhe1* null cells.

References

Van Haastert, P.J., and Devreotes, P.N. (2004). Chemotaxis: signalling the way forward. Nat Rev Mol Cell Biol *5*, 626-634. 10.1038/nrm1435.

Jin, T. (2011). GPCR-controlled chemotaxis in Dictyostelium discoideum. Wiley Interdiscip Rev Syst Biol Med *3*, 717-727. 10.1002/wsbm.143.

Murphy, P.M. (2002). International Union of Pharmacology. XXX. Update on chemokine receptor nomenclature. Pharmacol Rev *54*, 227-229. 10.1124/pr.54.2.227.

Jin, T., Xu, X., Fang, J., Isik, N., Yan, J., Brzostowski, J.A., and Hereld, D. (2009). How human leukocytes track down and destroy pathogens: lessons learned from the model organism Dictyostelium discoideum. Immunol Res *43*, 118-127. 10.1007/s12026-008-8056-7.

Jin, T., Xu, X., and Hereld, D. (2008). Chemotaxis, chemokine receptors and human disease. Cytokine *44*, 1-8. 10.1016/j.cyto.2008.06.017.

Kortholt, A., and van Haastert, P.J. (2008). Highlighting the role of Ras and Rap during Dictyostelium chemotaxis. Cell Signal *20*, 1415-1422. 10.1016/j.cellsig.2008.02.006.

Kumagai, A., Hadwiger, J.A., Pupillo, M., and Firtel, R.A. (1991). Molecular genetic analysis of two G alpha protein subunits in Dictyostelium. J Biol Chem *266*, 1220-1228.

Clapham, D.E., and Neer, E.J. (1993). New roles for G-protein beta gamma-dimers in transmembrane signalling. Nature *365*, 403-406. 10.1038/365403a0.

Charest, P.G., and Firtel, R.A. (2007). Big roles for small GTPases in the control of directed cell movement. Biochem J *401*, 377-390. 10.1042/BJ20061432.

Bos, J.L. (2005). Linking Rap to cell adhesion. Curr Opin Cell Biol *17*, 123-128. 10.1016/j.ceb.2005.02.009.

Lee, M.R., and Jeon, T.J. (2012). Cell migration: regulation of cytoskeleton by Rap1 in Dictyostelium discoideum. J Microbiol *50*, 555-561. 10.1007/s12275-012-2246-7.

Jeon, T.J., Lee, D.J., Merlot, S., Weeks, G., and Firtel, R.A. (2007). Rap1 controls cell adhesion and cell motility through the regulation of myosin II. J Cell Biol *176*, 1021-1033. 10.1083/jcb.200607072.

Park, B., Kim, H., and Jeon, T.J. (2018). Loss of RapC causes defects in cytokinesis, cell migration, and multicellular development of Dictyostelium. Biochem Biophys Res Commun *499*, 783-789. 10.1016/j.bbrc.2018.03.223.

Jeon, J., Kim, D., and Jeon, T.J. (2021). Opposite functions of RapA and RapC in cell adhesion and migration in Dictyostelium. Anim Cells Syst (Seoul) *25*, 203-210. 10.1080/19768354.2021.1947372.

Kim, D., Kim, W., and Jeon, T.J. (2021). Reversible function of RapA with the C-terminus of RapC in Dictyostelium. J Microbiol *59*, 848-853. 10.1007/s12275-021-1400-5.

Mun, H., Lee, M.R., and Jeon, T.J. (2014). RapGAP9 regulation of the morphogenesis and development in Dictyostelium. Biochem Biophys Res Commun *446*, 428-433. 10.1016/j.bbrc.2014.01.196.

Reshkin, S.J., Bellizzi, A., Caldeira, S., Albarani, V., Malanchi, I., Poignee, M., Alunni-Fabbroni, M., Casavola, V., and Tommasino, M. (2000). Na+/H+ exchanger-dependent intracellular alkalinization is an early event in malignant transformation and plays an essential role in the development of subsequent transformation-associated phenotypes. FASEB J *14*, 2185-2197. 10.1096/fj.00-0029com.

Hu, Y., Lou, J., Jin, Z., Yang, X., Shan, W., Du, Q., Liao, Q., Xu, J., and Xie, R. (2021). Advances in research on the regulatory mechanism of NHE1 in tumors. Oncol Lett *21*, 273. 10.3892/ol.2021.12534.

Brisson, L., Reshkin, S.J., Gore, J., and Roger, S. (2012). pH regulators in invadosomal functioning: proton delivery for matrix tasting. Eur J Cell Biol *91*, 847-860. 10.1016/j.ejcb.2012.04.004.

Dibrov, P., and Fliegel, L. (1998). Comparative molecular analysis of Na+/H+ exchangers: a unified model for Na+/H+ antiport? FEBS Lett *424*, 1-5. 10.1016/s0014-5793(98)00119-7.

Parent, C.A. (2004). Making all the right moves: chemotaxis in neutrophils and Dictyostelium. Curr Opin Cell Biol *16*, 4-13. 10.1016/j.ceb.2003.11.008.

Sasaki, A.T., and Firtel, R.A. (2006). Regulation of chemotaxis by the orchestrated activation of Ras, PI3K, and TOR. Eur J Cell Biol *85*, 873-895. 10.1016/j.ejcb.2006.04.007.

Patel, H., and Barber, D.L. (2005). A developmentally regulated Na-H exchanger in Dictyostelium discoideum is necessary for cell polarity during chemotaxis. J Cell Biol *169*, 321-329. 10.1083/jcb.200412145.

Gao, R., Zhao, S., Jiang, X., Sun, Y., Zhao, S., Gao, J., Borleis, J., Willard, S., Tang, M., Cai, H., et al. (2015). A large-scale screen reveals genes that mediate electrotaxis in Dictyostelium discoideum. Sci Signal *8*, ra50. 10.1126/scisignal.aab0562.

Robinson, K.R. (1985). The responses of cells to electrical fields: a review. J Cell Biol *101*, 2023-2027. 10.1083/jcb.101.6.2023.

Gao, R.C., Zhang, X.D., Sun, Y.H., Kamimura, Y., Mogilner, A., Devreotes, P.N., and Zhao, M. (2011). Different roles of membrane potentials in electrotaxis and chemotaxis of dictyostelium cells. Eukaryot Cell *10*, 1251-1256. 10.1128/EC.05066-11.

Mycielska, M.E., and Djamgoz, M.B. (2004). Cellular mechanisms of direct-current electric field effects: galvanotaxis and metastatic disease. J Cell Sci *117*, 1631-1639. 10.1242/jcs.01125.

van Duijn, B., and Vogelzang, S.A. (1989). The membrane potential of the cellular slime mold Dictyostelium discoideum is mainly generated by an electrogenic proton pump. Biochim Biophys Acta *983*, 186-192. 10.1016/0005-2736(89)90232-0.

Jeon, T.J., Gao, R., Kim, H., Lee, A., Jeon, P., Devreotes, P.N., and Zhao, M. (2019). Cell migration directionality and speed are independently regulated by RasG and Gbeta in Dictyostelium cells in electrotaxis. Biol Open *8*. 10.1242/bio.042457.

Pontel, L.B., Langenick, J., Rosado, I.V., Zhang, X.Y., Traynor, D., Kay, R.R., and Patel, K.J. (2016). Xpf suppresses the mutagenic consequences of phagocytosis in Dictyostelium. J Cell Sci *129*, 4449-4454. 10.1242/jcs.196337.

Cardelli, J. (2001). Phagocytosis and macropinocytosis in Dictyostelium: phosphoinositide-based processes, biochemically distinct. Traffic *2*, 311-320. 10.1034/j.1600-0854.2001.002005311.x.

Van Duijn, B., and Inouye, K. (1991). Regulation of movement speed by intracellular pH during Dictyostelium discoideum chemotaxis. Proc Natl Acad Sci U S A *88*, 4951-4955. 10.1073/pnas.88.11.4951.

Rougerie, P., Miskolci, V., and Cox, D. (2013). Generation of membrane structures during phagocytosis and chemotaxis of macrophages: role and regulation of the actin cytoskeleton. Immunol Rev *256*, 222-239. 10.1111/imr.12118.

Berridge, M.J., Lipp, P., and Bootman, M.D. (2000). The versatility and universality of calcium signalling. Nat Rev Mol Cell Biol *1*, 11-21. 10.1038/35036035.